Myocardial Blood Flow, Function, and Metabolism in Repetitive Stunning

Marcelo F. Di Carli, Petar Prcevski, Tajinder P. Singh, James Janisse, Joel Ager, Otto Muzik, and Richard Vander Heide

Division of Cardiology, Department of Internal Medicine; PET Center, Department of Pediatric Imaging; Center for Health Care Effectiveness Research; and Department of Pathology, Wayne State University School of Medicine, Detroit, Michigan

Myocardial hibernation refers to a state of persistent left ventricular dysfunction resulting from a chronically reduced blood flow, which is improved or reversed with revascularization. Increased glucose uptake in areas with reduced blood flow at rest on PET has been used successfully to diagnose hibernating myocardium. However, hibernation may represent persistent myocardial stunning resulting from repeated episodes of ischemia and reperfusion rather than from chronic underperfusion. We sought to determine the inter-relationship between blood flow, metabolism, and function in a canine model of repetitive myocardial stunning. **Methods:** Ten dogs underwent 4 sequential 5-min intervals of balloon occlusion of the anterior descending or circumflex arteries, each separated by 5 min of reperfusion. Regional blood flow, metabolism, and function were evaluated 3–4 h after reperfusion in all dogs and 24 h and 1 wk after reperfusion in 5 dogs. Regional wall motion was evaluated with echocardiography. Regional blood flow was assessed with radioactive microspheres and by [^{13}N]ammonia and PET. Measurements of oxidative metabolism and glucose uptake (during hyperinsulinemic–euglycemic clamping) were derived with [^{11}C]-acetate, FDG, and PET. **Results:** Regional wall motion was severely decreased after the 4 cycles of ischemia, remained impaired 24 h after reperfusion, and normalized after 1 wk. During reflow, blood flow in stunned regions was restored to near-normal levels (0.89 ± 0.07 versus 0.95 ± 0.07 mL/g/min, $P = 0.023$). However, glucose uptake in stunned regions was significantly decreased at 4 h (73% ± 5% of remote, $P < 0.001$), remained depressed after 24 h of reflow (83% ± 4% of remote, $P = 0.013$), and fully recovered at 1 wk (101% ± 10% of remote, $P = 0.88$). Similarly, oxidative metabolism in stunned regions was significantly decreased at 4 h (84% ± 2% of remote, $P < 0.001$) and at 24 h (90% ± 2% of remote, $P = 0.005$) and recovered to near-normal levels after 1 wk of reperfusion (97% ± 1% of remote, $P = 0.024$). The time course of change in postischemic dysfunction correlated with the recovery of oxidative metabolism ($r = 0.57$; $P = 0.009$). **Conclusion:** Myocardium subjected to repetitive stunning showed a prolonged yet reversible reduction in systolic function that was associated with a significant downregulation of glucose and oxidative metabolism despite restoration of normal myocardial blood flow. These findings suggest a unique metabolic adaptation in repetitive stunning that is different from that typically seen in clinical and experimental models of hibernation.

Key Words: stunning; blood flow; PET; ischemia; reperfusion

J Nucl Med 2000; 41:1227–1234

Myocardial hibernation refers to a state of persistent left ventricular dysfunction resulting from a chronic and sustained reduction in myocardial blood flow, which is improved or reversed with revascularization (*1*). This chronic downregulation in contractile function at rest is thought to reflect an endogenous protective mechanism whereby the heart reduces its oxygen demand to ensure myocyte survival. Although the original observations by Rahimtoola (*1*) proposed chronic and sustained hypoperfusion, recent studies in humans have suggested that hibernating segments have near-normal blood flow at rest but impaired coronary flow reserves (*2,3*). On the basis of these observations, investigators have proposed that chronic hibernation may actually result from repeated episodes of reversible ischemia (caused by a loss of coronary flow reserve) that ultimately lead to a state of persistent postischemic dysfunction (*2,3*).

Increased glucose use has been shown to exist in many clinical and experimental models of short-term hibernation (*4,5*). Increased glucose uptake in areas with reduced blood flow at rest (perfusion–metabolism mismatch) on PET has been used successfully for diagnosing hibernating myocardium in patients with left ventricular dysfunction (*4*). In contrast, a recent study using an animal model of repetitive myocardial stunning induced by brief episodes of low-flow ischemia failed to show an increase in glucose use (as seen in hibernation), at least early after the last ischemic cycle (*6*). However, little is known about the long-term relationship between the alterations in contractile function, flow, and metabolism in repetitive myocardial stunning.

The objective of this study was to characterize both the acute and the long-term abnormalities in regional myocardial blood flow and metabolism in repetitively stunned myocardium and to relate them to the alterations in postischemic left ventricular dysfunction.

Received Apr. 9, 1999; revision accepted Sep. 21, 1999.

For correspondence or reprints contact: Marcelo F. Di Carli, MD, Division of Cardiology, Harper Hospital, 3990 John R. Rd., Detroit, MI 48201.

MATERIALS AND METHODS

Animal Selection and Instrumentation

All experiments conformed to the guidelines of the U.S. National Institutes of Health (*7*). Ten healthy adult mongrel dogs of either sex, weighing 15–25 kg, were used. The dogs were anesthetized with morphine sulfate (1 mg/kg sulfur chloride) and sodium pentobarbital (25 mg/kg intravenous) and mechanically ventilated with a Harvard respirator (Harvard Apparatus, South Natick, MA) using room air. Anesthesia was maintained with intravenous morphine sulfate (0.5 mg/kg/h) and sodium pentobarbital (4 mg/kg/h). The same anesthetic agents and doses were used in the dogs that were re-evaluated 24 h and 1 wk after reperfusion. The left carotid artery was exposed, and an 8-French multipurpose Judkins coronary catheter was advanced through an arterial sheath into the ostium of the left anterior descending or circumflex coronary arteries. A balloon catheter was then passed through the guiding catheter and positioned in either vessel for sequential coronary occlusions. A 6-French pigtail catheter was advanced into the left ventricle through the right femoral artery for injection of radioactive microspheres. An additional catheter was introduced into the left femoral artery to obtain reference arterial blood samples during injection of the microspheres and to measure arterial blood pressure. Electrocardiography findings and blood pressure were monitored continuously throughout the procedure. After surgical preparation, at least 15 min were allowed for the dogs to reach a steady state.

Experimental Design

The general experimental protocol is summarized in Figure 1. Repetitive stunning was induced by 4 sequential 5-min intervals of occlusion of the left anterior descending or circumflex coronary arteries, each separated by 5 min of reperfusion. This protocol has been shown to induce regional contractile dysfunction without significant myocardial necrosis (*8*). Myocardial blood flow was measured with radioactive microspheres at baseline and midway into the fourth balloon occlusion in every animal. Regional systolic function was assessed at baseline, during each interval of occlusion, and 4 h after reperfusion in all animals. In 5 dogs, regional systolic function was also evaluated 24 h and 1 wk after reperfusion. Myocardial blood flow, oxidative metabolism, and glucose uptake were evaluated by PET 3–4 h after reperfusion in every animal and 24 h and 1 wk after reperfusion in 5 animals.

Echocardiography

Regional systolic function was assessed by 2-dimensional echocardiography (model 880; Aloka Co., Ltd., Tokyo, Japan). Short-axis views of the left ventricle were obtained with the dogs positioned on their right side and the transducer applied to the chest wall from below the imaging table. Mid short-axis images at the papillary muscle level were obtained for comparison with the PET images and microsphere data (Fig. 2). The location, extent, and severity of a wall motion abnormality were determined visually by 2 observers without knowledge of the status of the myocardium being evaluated. Segmental wall motion was visually assessed using a 0–3 scale: 0 = akinesis, 1 = severe hypokinesis, 2 = mild hypokinesis, and 3 = normal.

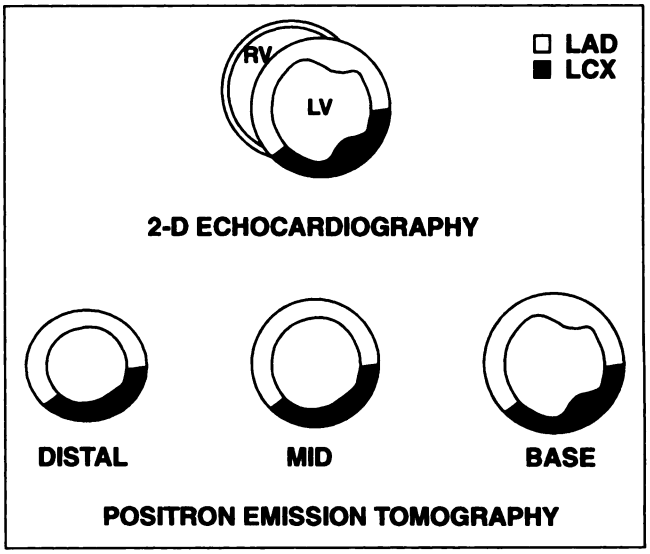

FIGURE 2. Diagram of correspondence between short-axis 2-dimensional (2-D) echocardiographic images and PET images. LAD = left anterior descending artery; LCX = left circumflex artery; LV = left ventricle; RV = right ventricle.

Microsphere Blood Flow

Radioactive microspheres (New England Nuclear, Boston, MA) labeled with ^{46}Sc, ^{57}Co, or ^{113}Sn were used to measure regional myocardial blood at baseline and during the fourth coronary occlusion. For each time point, 1–2 million microspheres were injected into the left ventricle through the pigtail catheter during a 20-s period, followed by a 10-mL saline flush. Beginning just before and continuing for 90 s after the injection of microspheres, reference arterial blood samples were withdrawn from the femoral artery at a rate of 7.75 mL/min.

At the end of the experiment, the index coronary artery (i.e., left anterior descending or circumflex) was ligated at the site of balloon occlusions, and 5 mL Superimperse (Ciba Geigy, Glensfalls, NY) blue dye were injected into the left atrial appendage to delineate the ischemic and nonischemic myocardium. The animals were then killed by intravenous injection of a concentrated potassium chloride solution under deep anesthesia. After arrest, the heart was excised and the left ventricle was cut into a series of approximately 1-cm-thick short-axis slices. Three slices distal to the coronary

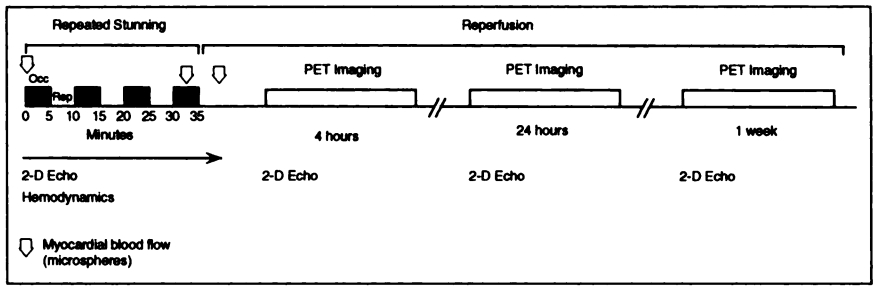

FIGURE 1. Diagram of experimental protocol. 2-D Echo = 2-dimensional echocardiography.

occlusion were selected for further analysis. In each slice, 2–3 segments (~1 g/each) were cut from the ischemic and normal remote zones and subdivided into subendocardial and subepicardial halves for blood flow measurements. Microsphere radioactivity in tissue and blood was then measured in a γ counter (Cobra II; Packard Instrument Co., Meriden, CT) with correction for overlap of isotopic spectra. Myocardial blood flow, expressed as mL/min/g, was calculated according to the following formula: tissue flow = (tissue counts)(reference blood flow)/reference blood counts.

PET

PET was used to evaluate regional myocardial blood flow, oxidative metabolism, and glucose use, using [^{13}N]ammonia, [^{11}C]acetate, and FDG, respectively. Imaging was performed using a whole-body PET scanner (EXACT HR; CTI/Siemens, Inc., Knoxville, TN), which acquires 47 contiguous transaxial planes with an image resolution of 3.6 ± 0.23 mm full width at half maximum (FWHM) in-plane and 3.5 ± 0.18 mm FWHM in the axial direction. The scanner has an interplane spacing of 3.125 mm and covers a 15-cm axial field of view. The images were reconstructed using a Hanning filter with a 1.10 cycle/cm cutoff frequency, resulting in an effective resolution of 6 mm FWHM.

Imaging Protocol. A 15-min transmission scan was acquired for correction of photon attenuation. Beginning with the intravenous bolus administration of [^{13}N]ammonia (10.6 MBq/kg), serial images were acquired for 20 min (12 images for 10 s each, 3 for 60 s, and 3 for 300 s). Thirty minutes later, an intravenous dose of [^{11}C]acetate (10.6 MBq/kg) was administered, and serial images were acquired for 30 min (12 images for 10 s each, 8 for 30 s, 4 for 60 s, 2 for 300 s, and 1 for 600 s). Sixty minutes later, a dose of FDG (5.2 MBq/kg) was administered intravenously, and images were recorded for 54 min (8 images for 15 s each, 4 for 30 s, 2 for 300 s, and 4 for 600 s).

Standardization of substrate availability for measurement of myocardial glucose uptake was performed by the insulin clamping technique (*9*), which was started after completion of the [^{11}C]-acetate images. Briefly, serum insulin was increased for 120 min using a primed continuous infusion of insulin (1 mU/kg/min). During hyperinsulinemia, normoglycemia was maintained using a variable rate infusion of 20% glucose adjusted according to the plasma glucose concentration, which was measured every 5 min from arterial blood. FDG was injected 50–60 min after the start of insulin clamping.

Analysis of PET Data. In each study, the 47 tomographic slices were reoriented into 12 short-axis slices extending from the apex to the base of the left ventricle. To quantify regional myocardial blood flow, regions of interest (ROIs) encompassing the ischemic and normal remote zones were automatically assigned to each of 4 midventricular short-axis slices of the [^{13}N]ammonia images. Assignment of sectorial ROIs is based on radial activity profiles with a blood volume fraction of 50%–60%, which allows incorporation of in-plane partial-volume effects and blood-to-tissue cross-contamination into the model equation (*10*). An additional small circular ROI was manually placed in the center of the left ventricular blood pool to obtain the arterial input function. The ROIs were then copied to the entire sequence of [^{13}N]ammonia images, and regional myocardial tissue and blood-pool time–activity curves were obtained. In each myocardial zone (i.e., ischemic and remote), a single time–activity curve was obtained by averaging the corresponding [^{13}N]ammonia data in adjacent ventricular planes. The curves were then fitted with a previously validated 3-compartment tracer kinetic model (*11*).

The same ROIs (as for the [^{13}N]ammonia images) were automatically assigned to each of 4 midventricular short-axis slices of the [^{11}C]acetate images to quantify the regional rate of oxidative metabolism. To ensure that the placement of these regions was identical, the same angle on the circumferential profile served as the starting point for the ROIs on each of the 3 or 9 sets of images studied in each dog. The ROIs were then copied to the entire sequence of [^{11}C]acetate images, and regional myocardial tissue time–activity curves were obtained. In each myocardial zone, a single time–activity curve was obtained by averaging corresponding data in adjacent ventricular planes. Regional rates of oxidative metabolism were estimated from the rate of clearance of [^{11}C]-acetate from myocardium, which has been shown to correlate closely with myocardial oxygen consumption (*12*). The tissue clearance rate, defined as k, was determined by monoexponential least squares fitting of the linear portion of the [^{11}C]acetate myocardial time–activity curve.

The regional rate of glucose use was quantified by automatically assigning identical ROIs to each of 4 midventricular short-axis slices of the FDG images. An additional small circular ROI was manually placed in the center of the left ventricular blood pool to obtain the arterial input function. The ROIs were then copied to the entire sequence of FDG images, and regional myocardial tissue and blood-pool time–activity curves were obtained. In each zone, a single time–activity curve was obtained by averaging corresponding data in adjacent ventricular planes. Regional rates of myocardial glucose use were quantified using a modified Patlak graphic analysis (*13*). To correct for the loss of radioactivity in the myocardium caused by partial-volume effects, time–activity curves were multiplied by a recovery factor derived from geometric representation of the myocardium, which takes into account the wall thickness as well as the FWHM of the PET system (*14*).

Statistical Analysis

Data are presented as mean ± SEM. Differences between stunned and remote myocardial regions were assessed using a paired Student *t* test. The time course of changes in postischemic dysfunction were investigated using a single-factor within-subjects ANOVA and a modified Bonferroni test to compare each time with the baseline. The Greenhouse-Geisser correction was used for the overall analysis to correct for any sphericity violation (*15*). Linear regression analysis was performed by least squares fitting. An α of 0.05 was used to define statistical significance. A P less than 0.10 was considered to indicate trends toward significance.

RESULTS

Hemodynamic Parameters

During the fourth coronary occlusion, a decrease in systolic and mean arterial blood pressure occurred, with a compensatory increase in heart rate. These parameters returned to baseline values after 20 min of reperfusion. No significant changes were observed in left ventricular pressure (Table 1).

Time Course of Postischemic Dysfunction

Regional systolic function decreased significantly during the first coronary occlusion, as reported previously. No

TABLE 1
Hemodynamic Parameters During Repeated Coronary Occlusions

Hemodynamic measure	Baseline	Fourth CO	30-min AR
Heart rate (bpm)	109 ± 6	129 ± 6	105 ± 6
Systolic BP (mm Hg)	173 ± 6	159 ± 8	161 ± 7
Mean arterial BP (mm Hg)	125 ± 4	116 ± 5	118 ± 4
LVEDP (mm Hg)	5 ± 1	7 ± 1	5 ± 1

CO = coronary occlusion; AR = after reperfusion; BP = blood pressure; LVEDP = left ventricular end-diastolic pressure.
Values are expressed as mean ± SEM.

further reductions in regional systolic function were observed with subsequent coronary occlusions (occlusions 2–4). Regional systolic function remained depressed 24 h after reperfusion and normalized after 1 wk (Fig. 3). Using the Greenhouse-Geisser correction, statistical analysis revealed a significant difference in systolic function over time ($P < 0.002$). Using a modified Bonferroni test, all time points except for 1 wk were significantly different from the baseline measure ($P < 0.05$).

Regional Changes in Myocardial Blood Flow

The changes in regional myocardial blood flow are illustrated in Figure 4. At baseline, myocardial blood flow was similar in remote and stunned myocardial regions. During the fourth coronary occlusion, subendocardial blood flow in the stunned region was significantly lower than in remote myocardium (0.28 ± 0.15 versus 1.11 ± 0.14 mL/min/g, $P = 0.001$). Subepicardial blood flow in the stunned region was also lower than in remote myocardium, but it did not reach statistical significance (0.48 ± 0.22 versus 0.90 ± 0.11 mL/min/g, $P = 0.11$). At 30 min after reperfusion, blood flow in stunned regions was restored and similar to that in remote myocardium. Blood flow in the stunned regions then deteriorated, although only modestly, at 4 h after reperfusion (0.89 ± 0.07 versus 0.95 ± 0.06 mL/g/min in remote myocardium, $P = 0.023$). However, blood flow in stunned myocardium was restored to near-normal levels at 24 h and 1 wk after reperfusion.

Regional Changes in Myocardial Metabolism

Myocardial Glucose Use. The time course of change in myocardial glucose use is summarized in Figures 5 and 6. Four hours after reperfusion, glucose use in stunned myocardium was significantly reduced to 73% ± 5% of remote myocardium ($P < 0.001$) (Table 2). Twenty-four hours after reperfusion, glucose use in the stunned regions remained depressed (83% ± 4% of remote myocardium, $P = 0.013$). Glucose use in stunned myocardium was restored to control levels after 1 wk of reperfusion.

Myocardial Oxidative Metabolism. The time course of change in myocardial oxidative metabolism is illustrated in Figures 5 and 6. Stunned myocardium also showed a modest but significant reduction in oxidative metabolism at 4 h (84% ± 2% of remote myocardium, $P < 0.001$) and 24 h (90% ± 2% of remote myocardium, $P = 0.005$) after reperfusion. One week after reperfusion, oxidative metabolism in stunned myocardium was restored to near-normal levels. The recovery of oxidative metabolism over time correlated with the time course of change in postischemic dysfunction ($r = 0.57$; $P = 0.009$).

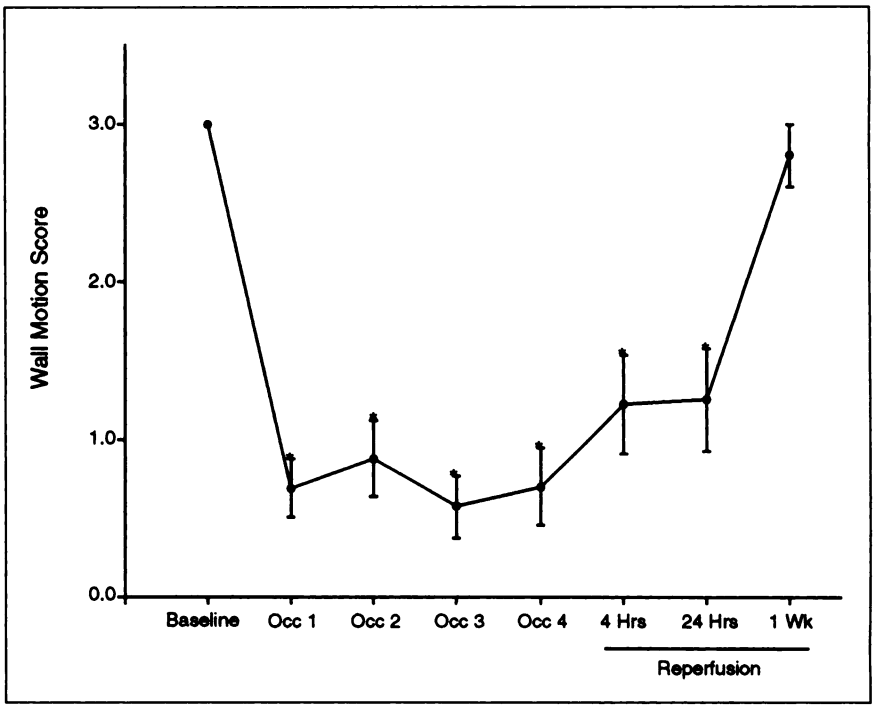

FIGURE 3. Graph shows changes in regional systolic function (wall motion score) in stunned myocardium during 4 coronary occlusions (Occ) and at 4 h, 24 h, and 1 wk after reperfusion. Data are mean ± SEM. *$P < 0.01$ versus baseline.

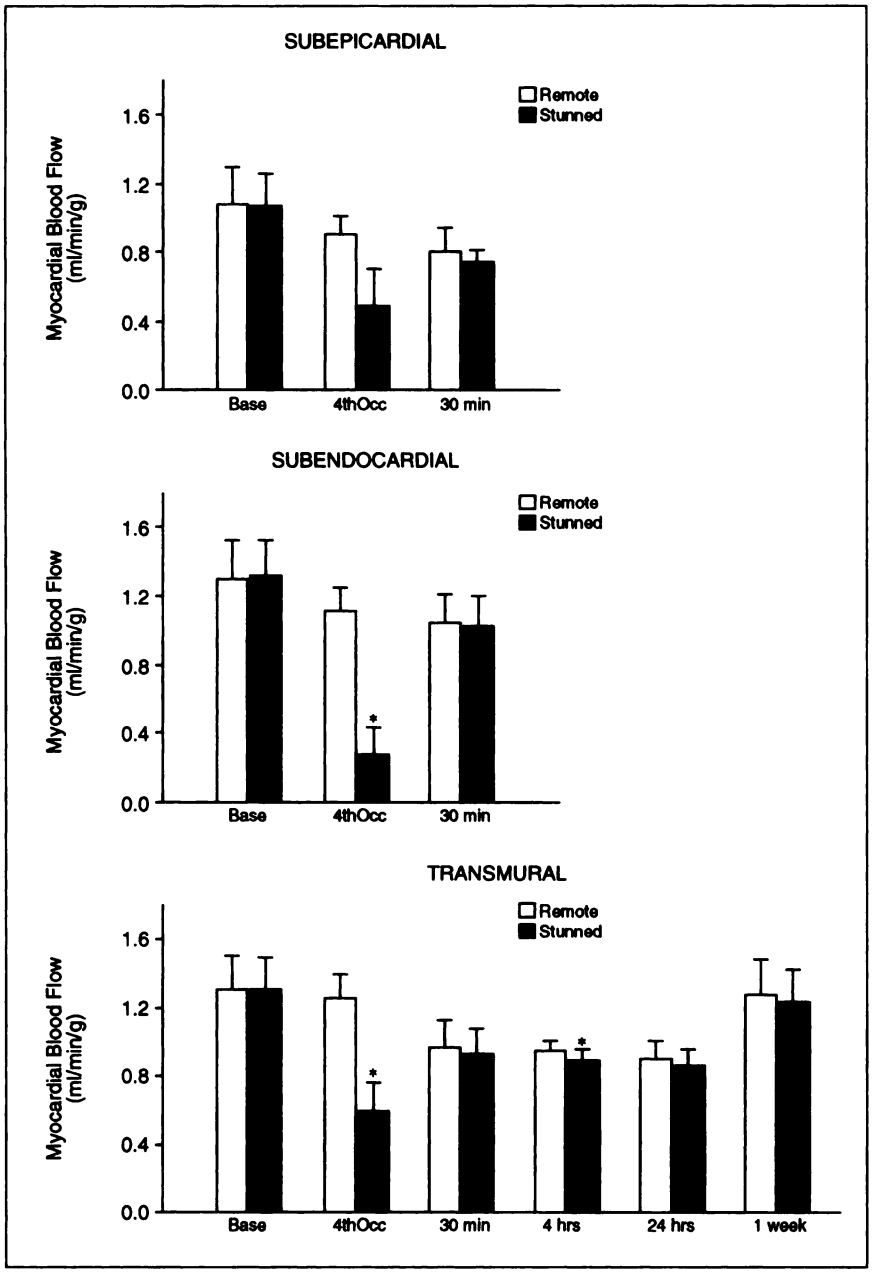

FIGURE 4. Bar graph shows changes in myocardial blood flow during ischemia and reperfusion. Radioactive microspheres were used to measure blood flow at baseline (Base), during fourth coronary occlusion (4thOcc), and at 30 min after reperfusion. PET with [^{13}N]ammonia as flow tracer was used to measure blood flow at 4 h, 24 h, and 1 wk after reperfusion. Data are mean ± SEM.

DISCUSSION

Myocardial hibernation was first described in humans as a chronic downregulation of contractile function caused by a sustained decreased in myocardial blood flow, with preserved viability that recovers after revascularization (*1*). However, recent studies have suggested that chronic hibernation may actually result from repeated episodes of reversible ischemia (caused by a loss of coronary flow reserve), ultimately leading to a state of persistent postischemic dysfunction (i.e., stunning) (*2,3*). Whatever the nature of the flow reduction (sustained or intermittent), hibernation as defined clinically is associated with important alterations in myocardial metabolism. These alterations include decreased oxygen consumption and increased glucose uptake as shown by the perfusion–metabolism mismatch pattern on PET (*4,16*).

The purpose of this study was to characterize the acute and the long-term alterations in flow, metabolism, and function that occur in a canine model of repetitive stunning. The results show that repeated, brief episodes of severe myocardial ischemia produced a prolonged alteration in regional contractile function, which was associated with a persistent reduction of myocardial metabolism. For example, after 4 h of reperfusion, regional blood flow in stunned myocardium had already returned to near-normal values. However, postischemic myocardium showed a 16% reduction in oxidative metabolism after 4 h of reperfusion, which remained depressed at 24 h and recovered to near-

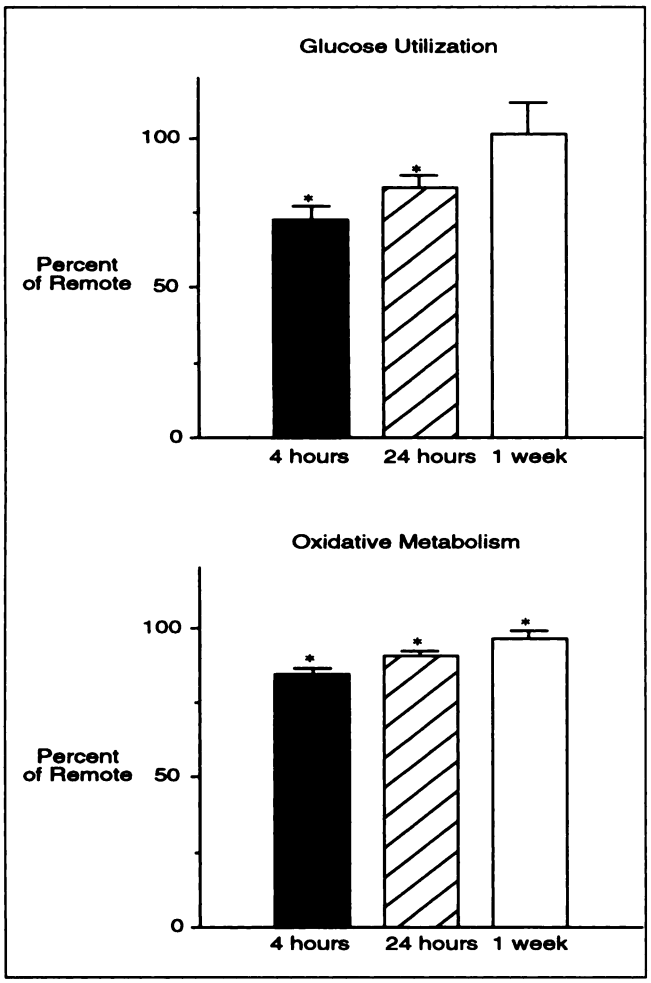

FIGURE 5. Bar graph shows time course of change in myocardial glucose use and oxidative metabolism obtained from FDG and [^{11}C]acetate kinetics at 4 h, 24 h, and 1 wk after reperfusion. Data are mean ± SEM.

normal levels within 1 wk of reperfusion. The time course of change in regional postischemic contractile dysfunction correlated significantly with the changes in regional oxidative metabolism.

Similarly, although blood flow had returned to normal, stunned myocardium showed a 27% reduction in glucose use 4 h after reperfusion. Glucose metabolism improved only partially after 24 h of reflow and fully recovered to control levels within 1 wk of reperfusion. These results contrast with previous clinical and experimental studies of myocardial hibernation, which reported an increase in glucose use despite reduced myocardial blood flow (*4*). Thus, our data indicate that the metabolic alterations after repetitive stunning are different from those typically associated with hibernation and suggest that the metabolic adaptations occurring in repetitive stunning and hibernation may occur through different cellular and subcellular mechanisms.

Model of Repetitive Myocardial Stunning

In patients with stable coronary artery disease, repetitive myocardial stunning can result from repeated episodes of ischemia and reperfusion caused by increases in oxygen demand in the setting of an impaired coronary vasodilator reserve caused by severe flow-limiting coronary stenoses (*2*). In patients with unstable coronary syndromes, myocardial stunning can result from transient episodes of coronary occlusion followed by reperfusion caused by thrombotic vessel occlusion at the site of plaque rupture (*17*). The stunning can also result from vasoconstriction caused by endothelial dysfunction and release of vasoactive substances by platelets (*18,19*). The purpose of this study was to assess the changes in myocardial blood flow, function, and metabolism in repetitive stunning using a closed-chest canine model of coronary occlusion and reperfusion. This model of repetitive stunning may apply only to patients with severe coronary stenoses, especially but not exclusively those presenting with unstable coronary syndromes.

Relationship Between Current Results and Previous Studies

The observed reduction in glucose uptake in stunned myocardium during early reperfusion (3–4 h) is consistent with previous reports (*20–23*). However, our results showed that regional glucose use in postischemic myocardium remained impaired at 24 h and recovered to normal levels only within 1 wk of reperfusion. This result differs from those of previous studies, perhaps because of differences in experimental design (*20–22*). In our study, changes in regional glucose uptake were assessed during hyperinsulinemic–euglycemic clamping to standardize the dietary state of the animals. This protocol has been shown to reduce the normal physiologic heterogeneity in glucose uptake in normal myocardium during fasting conditions (*21,24*).

The mechanisms by which stunned myocardium after multiple cycling of ischemia and reperfusion showed a prolonged reduction of glucose use cannot be determined from this study. Oxidation of all major substrates including glucose is depressed after reperfusion, and nonglucose substrates are preferred for oxidative metabolism. Indeed, previous studies have shown that reperfused myocardium has a strong preference for and aerobic use of fatty acids during reflow (*25,26*). Further, carbohydrate use for oxidative metabolism during reflow is significantly reduced (*23,27*). One possible mechanism for the reduced glucose uptake in reperfused tissue is a decrease in the activity of key regulatory enzymes of the glycolytic pathway because of shifting levels of metabolites after ischemia and reperfusion (*28*). Another possibility is that multiple cycling of ischemia and reperfusion or their metabolic byproducts may have decreased glucose uptake by decreasing the number of insulin receptors or their sensitivity to insulin (*29*), or by altering the process in which insulin signals GLUT-4 translocation (*30,31*), or both.

The time course of change in oxidative metabolism in stunned myocardium was similar to that reported for other ischemia–reperfusion protocols (*32,33*). More specifically, the linear correlation between the improvement in postischemic dysfunction and the restoration of oxidative metabo-

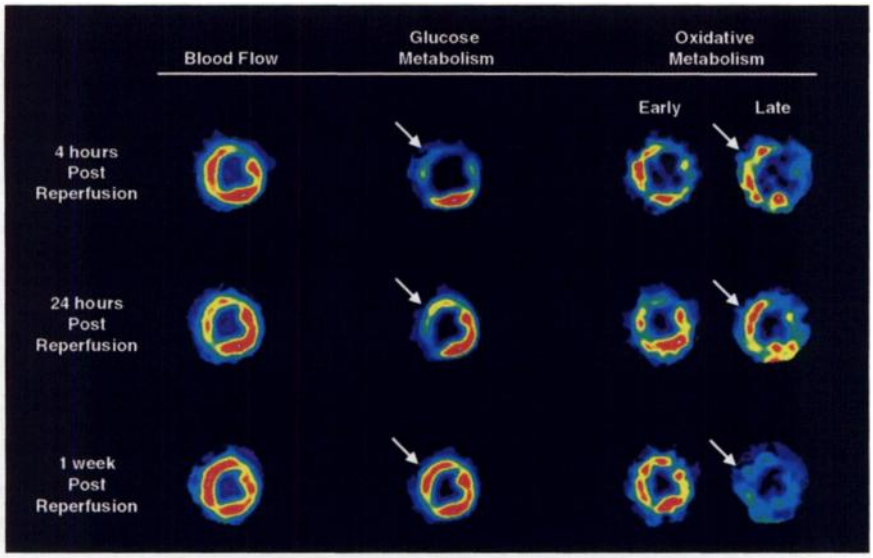

FIGURE 6. Mid short-axis PET images obtained after reperfusion of dog heart. Images are oriented with anterior wall at top, inferior wall at bottom, interventricular septum to left, and lateral wall to right. Each image is scaled to its own maximum. Early phase of oxidative metabolism ([^{11}C]acetate) denotes delivery of tracer to myocardium, whereas late phase represents regional washout of tracer (oxidation). In images obtained 3–4 h after reperfusion (top row), blood flow (left) was near normal in stunned regions (anterior and anteroseptal walls). However, stunned regions showed severely reduced glucose uptake (arrow) and slow clearance of [^{11}C]acetate (impaired oxidation, arrow) relative to normal myocardium (lateral wall). In images obtained 1 d after reperfusion (middle row), myocardial perfusion in stunned myocardium is near normal, glucose uptake remains depressed (arrow), and oxidative metabolism is still decreased (arrow) compared with normal myocardium. In images obtained 1 wk after reperfusion (bottom row), stunned regions (arrows) are homogeneous with remote regions.

lism observed in this study is consistent with previous reports (*33*). Similar to us, Buxton et al. (*32*) showed a 25% reduction in oxidative metabolism in stunned myocardium during early reperfusion, which remained impaired at 24 h and recovered by 1 mo after reperfusion. Weinheimer et al. (*33*) reported similar findings. Therefore, the current data further support the notion that restoration of oxidative metabolism is a necessary prerequisite for full recovery of postischemic ventricular dysfunction.

CONCLUSION

Myocardium stunned with repeated episodes of brief ischemia and reperfusion shows prolonged postischemic dysfunction despite a near-complete restoration of regional blood flow. Both oxidative metabolism and glucose use were reduced early after reperfusion (3–4 h), remained impaired at 24 h, and recovered within 1 wk. Furthermore, the time course of change in myocardial metabolism paralleled that of postischemic contractile dysfunction. On the basis of these data, we suggest that in repetitive myocardial stunning, a unique metabolic adaptation occurs that is different from the adaptation typically described in clinical and experimental models of myocardial hibernation.

ACKNOWLEDGMENTS

The authors thank Galina Rabkin, Teresa Jones, and Benjamin Lathrop for expert technical assistance with the

TABLE 2
Changes in Myocardial Glucose Use and Oxidative Metabolism After Reperfusion

	4 h		24 h		1 wk	
Parameter	Mean ± SD	% of remote	Mean ± SD	% of remote	Mean ± SD	% of remote
MRGLc (μmol/min/g)						
Remote	0.61 ± 0.15	73 ± 5%	0.75 ± 0.12	83 ± 4%	0.55 ± 0.07	101 ± 10%
Stunned	0.43 ± 0.09*		0.61 ± 0.07†		0.57 ± 0.11	
MVO_2 (k/min)						
Remote	0.13 ± 0.02	84 ± 2%	0.13 ± 0.01	90 ± 2%	0.17 ± 0.02	96 ± 1%
Stunned	0.11 ± 0.02*		0.12 ± 0.01*		0.17 ± 0.02*	

*$P < 0.05$ vs. remote.
†$P = 0.067$ vs. remote.
MRGLc = myocardial glucose metabolism; MVO_2 = myocardial oxidative metabolism.

PET studies and Thomas Mangner and Pulak Chakroborty for reliably supplying the radiopharmaceuticals.

REFERENCES

1. Rahimtoola SH. The hibernating myocardium. *Am Heart J.* 1989;117:211–221.
2. Vanoverschelde JL, Wijns W, Depre C, et al. Mechanisms of chronic regional postischemic dysfunction in humans: new insights from the study of noninfarcted collateral-dependent myocardium. *Circulation.* 1993;87:1513–1523.
3. Marinho NV, Keogh BE, Costa DC, Lammerstma AA, Ell PJ, Camici PG. Pathophysiology of chronic left ventricular dysfunction: new insights from the measurement of absolute myocardial blood flow and glucose utilization. *Circulation.* 1996;93:737–744.
4. Tillisch J, Brunken R, Marshall R, et al. Reversibility of cardiac wall-motion abnormalities predicted by positron tomography. *N Engl J Med.* 1986;314:884–888.
5. Liedtke AJ, Renstrom B, Nellis SH, Hall JL, Stanley WC. Mechanical and metabolic functions in pig hearts after 4 days of chronic coronary stenosis. *J Am Coll Cardiol.* 1995;26:815–825.
6. Hacker TA, Renstrom B, Nellis SH, Liedtke AJ. Effect of repetitive stunning on myocardial metabolism in pig hearts. *Am J Physiol.* 1997;273:H1395–H1402.
7. Institute of Laboratory Animal Resources Commission of Life Sciences, National Research Council. *Guide for the Care and Use of Laboratory Animals.* Washington, DC: National Academy Press; 1996.
8. Murry CE, Jennings RB, Reimer KA. Preconditioning with ischemia: a delay of lethal cell injury in ischemic myocardium. *Circulation.* 1986;74:1124–1136.
9. Nuutila P, Koivisto VA, Knuuti J, et al. Glucose-free fatty acid cycle operates in human heart and skeletal muscle in vivo. *J Clin Invest.* 1992;89:1767–1774.
10. Hutchins GD, Caraher JM, Raylman RR. A region of interest strategy for minimizing resolution distortions in quantitative myocardial PET studies. *J Nucl Med.* 1992;33:1243–1250.
11. Muzik O, Beanlands RS, Hutchins GD, Mangner TJ, Nguyen N, Schwaiger M. Validation of nitrogen-13-ammonia tracer kinetic model for quantification of myocardial blood flow using PET. *J Nucl Med.* 1993;34:83–91.
12. Armbrecht JJ, Buxton DB, Schelbert HR. Validation of [1–11C]acetate as a tracer for noninvasive assessment of oxidative metabolism with positron emission tomography in normal, ischemic, postischemic, and hyperemic canine myocardium. *Circulation.* 1990;81:1594–1605.
13. Gambhir SS, Schwaiger M, Huang SC, et al. Simple noninvasive quantification method for measuring myocardial glucose utilization in humans employing positron emission tomography and fluorine-18 deoxyglucose. *J Nucl Med.* 1989;30:359–366.
14. Gambhir SS. *Quantification of the Physical Factors Affecting the Tracer Kinetic Modelling of Cardiac Positron Emission Tomography Data* [dissertation]. Los Angeles, CA: University of California; 1990.
15. Geisser S, Greenhouse SW. An extension of Box's results on the use of the F distribution in multivariate analysis. *Ann Math Statistics.* 1958;29:885–891.
16. Gropler RJ, Siegel BA, Sampathkumaran K, et al. Dependence of recovery of contractile function on maintenance of oxidative metabolism after myocardial infarction. *J Am Coll Cardiol.* 1992;19:989–997.
17. Fuster V, Badimon L, Cohen M, Ambrose JA, Badimon JJ, Chesebro J. Insights into the pathogenesis of acute ischemic syndromes. *Circulation.* 1988;77:1213–1220.
18. Hackett D, Davies G, Chierchia S, Maseri A. Intermittent coronary occlusion in acute myocardial infarction: value of combined thrombolytic and vasodilator therapy. *N Engl J Med.* 1987;317:1055–1059.
19. Bogaty P, Hackett D, Davies G, Maseri A. Vasoreactivity of the culprit lesion in unstable angina. *Circulation.* 1994;90:5–11.
20. Buxton DB, Schelbert HR. Measurement of regional glucose metabolic rates in reperfused myocardium. *Am J Physiol.* 1991;261:H2058–H2068.
21. Schwaiger M, Schelbert HR, Ellison D, et al. Sustained regional abnormalities in cardiac metabolism after transient ischemia in the chronic dog model. *J Am Coll Cardiol.* 1985;6:336–347.
22. McFalls EO, Baldwin D, Marx D, Fashingbauer P, Ward H. Temporal changes in function and regional glucose uptake within stunned porcine myocardium. *J Nucl Med.* 1996;37:2006–2010.
23. Renstrom B, Nellis SH, Liedtke AJ. Metabolic oxidation of glucose during early myocardial reperfusion. *Circ Res.* 1989;65:1094–1101.
24. Buxton DB, Nienaber CA, Luxen A, et al. Noninvasive quantitation of regional myocardial oxygen consumption in vivo with [1–11C]acetate and dynamic positron emission tomography. *Circulation.* 1989;79:134–142.
25. Myears DW, Sobel BE, Bergmann SR. Substrate use in ischemic and reperfused canine myocardium: quantitative considerations. *Am J Physiol.* 1987;253:H107–H114.
26. Liedtke AJ, DeMaison L, Eggleston AM, Cohen LM, Nellis SH. Changes in substrate metabolism and effects of excess fatty acids in reperfused myocardium. *Circ Res.* 1988;62:535–542.
27. Liedtke AJ, Renstrom B, Hacker TA, Nellis SH. Effects of moderate repetitive ischemia on myocardial substrate utilization. *Am J Physiol.* 1995;269:H246–H253.
28. Kobayashi K, Neely JR. Effects of ischemia and reperfusion on pyruvate dehydrogenase activity in isolated rat hearts. *J Mol Cell Cardiol.* 1983;15:359–367.
29. Dodds K, Lamb P, Pentecost B, Nattrass M. Erythrocyte insulin receptors following myocardial infarction in non-diabetic subjects. *Ann Clin Biochem.* 1986;23:657–660.
30. Harada K, Maekawa T, Abu Shama KM, Yamashima T, Yoshida K. Translocation and down-regulation of protein kinase C-alpha, -beta, and -gamma isoforms during ischemia-reperfusion in rat brain. *J Neurochem.* 1999;72:2556–2564.
31. Shepherd PR, Kahn BB. Glucose transporters and insulin action: implications for insulin resistance and diabetes mellitus. *N Engl J Med.* 1999;341:248–257.
32. Buxton DB, Mody FV, Krivokapich J, Phelps ME, Schelbert HR. Quantitative assessment of prolonged metabolic abnormalities in reperfused canine myocardium. *Circulation.* 1992;85:1842–1856.
33. Weinheimer CJ, Brown MA, Nohara R, Perez JE, Bergmann SR. Functional recovery after reperfusion is predicated on recovery of myocardial oxidative metabolism. *Am Heart J.* 1993;125:939–949.